

Exploring the potential of Sentinel-2A satellite data for aboveground biomass estimation in fragmented Himalayan subtropical pine forest

Mobushir Riaz KHAN¹  <https://orcid.org/0000-0002-6533-0743>; e-mail: mobkhan@csu.edu.au; mobushir.riaz@icloud.com

Iftikhar Ahmad KHAN²  <https://orcid.org/0000-0002-8930-9658>; e-mail: ik188960@gmail.com

Muhammad Hasan Ali BAIG^{3*}  <https://orcid.org/0000-0001-6513-4921>;  e-mail: mhasanbaig@uaar.edu.pk

LIU Zheng-jia⁴  <https://orcid.org/0000-0002-4577-446X>; e-mail: liuzj@igsnrr.ac.cn

Muhammad Irfan ASHRAF⁵  <https://orcid.org/0000-0003-4794-3754>; e-mail: irfanashraf@uaar.edu.pk & drirfancanada@gmail.com

* Corresponding author

¹ School of Environmental Science, Charles Sturt University, Albury, NSW 2640, Australia

² Institute of Geo-information & Earth Observation, Arid Agriculture University Rawalpindi, Pakistan & (ii) Department of Forest, Azad Jammu & Kashmir Muzaffarabad-13100, Pakistan

³ Institute of Geo-information & Earth Observation (IGEO), PMAS Arid Agriculture University Rawalpindi 46300, Pakistan

⁴ Institute of Geographic Sciences and Natural Resources Research, Chinese Academy of Sciences, Beijing 100101, China

⁵ Department of Forestry & Range Management, PMAS Arid Agriculture University Rawalpindi 46300, Pakistan

Citation: Khan MR, Khan IA, Baig MHA, et al. (2020) Exploring the potential of sentinel-2A satellite data for aboveground biomass estimation in fragmented Himalayan subtropical pine forest. Journal of Mountain Science 17(12). <https://doi.org/10.1007/s11629-019-5968-8>

© Science Press, Institute of Mountain Hazards and Environment, CAS and Springer-Verlag GmbH Germany, part of Springer Nature 2020

Abstract: The Sentinel-2A satellite having embedded advantage of red edge spectral bands offers multispectral imageries with improved spatial, spectral and temporal resolutions as compared to the other contemporary satellites providing medium resolution data. Our study was aimed at exploring the potential of Sentinel-2A imagery to estimate Above Ground Biomass (AGB) of Subtropical Pine Forest in Pakistan administered Kashmir. We developed an AGB predictive model using field inventory and Sentinel 2A based spectral and textural parameters along with topographic features derived from ALOS Digital Elevation Model (DEM). Field inventory data was collected from 108 randomly distributed plots (0.1 ha each) across the study area. The stepwise

linear regression method was employed to investigate the potential relationship between field data and corresponding satellite data. Biomass and carbon mapping of the study area was carried out through established AGB estimation model with R (0.86), R^2 (0.74), adjusted R^2 (0.72) and RMSE value of 33 t/ha. Our results showed that first order textures (mean, standard deviation and variance) significantly contributed in AGB predictive modeling while only one spectral band ratio made contribution from spectral domain. Our study leads to the conclusion that Sentinel-2A optical data is a potential source for AGB estimation in subtropical pine forest of the area of interest with added benefit of its free of cost availability, higher quality data and long-term continuity that can be utilized for biomass carbon distribution mapping in the resource constraint study area for sustainable forest management.

Received: 31-Dec-2019

1st Revision: 21-May-2020

2nd Revision: 09-Jul-2020

Accepted: 18-Aug-2020

Keywords: Field inventory; Forest Biomass; Sentinel 2A; AGB Modelling; Spectral features; Textures

Introduction

Global climate change resulting from Green House Gases (GHGs) emissions is one of the most serious environmental issues that we are confronted with today (Cheng et al. 2015) and it may severely impact the natural ecosystems (Ravindranath and Sathaye 2002). It is believed that increasing concentration of CO₂ (a prominent greenhouse gas) is primarily responsible for change in global climate (Yohannes et al. 2015; Dar and Sundarapandian 2015). An approach to reduce atmospheric concentration of carbon dioxide through forest ecosystems has gained attention because it is considered as an environment friendly, cost effective and a safe way to capture and store the substantial amounts of carbon from the atmosphere (Vikrant and Chauhan 2014). Forests which cover nearly 30% of global land surface (Keenan et al. 2015) can play a significant role in climate change mitigation (Federici et al. 2015). The role of forests in the context of climate change has been extensively discussed in United Nations Framework Convention on Climate Change (UNFCCC) (Keenan et al. 2015) and their unique role as carbon sinks was recognized under Kyoto Protocol (FAO 2005). Forest ecosystems can sequester and store more carbon than any other terrestrial ecosystem and tend to offer a natural brake on climate change (Gibbs et al. 2007) and can help mitigate the impacts of climate change (Cheng et al. 2015). Forests sequester atmospheric CO₂ through photosynthesis and store it as wood biomass (Kumar et al. 2016) where approximately 50% of biomass is carbon (Goetz et al. 2009). Since biomass can be readily converted into carbon, therefore, its role becomes important in carbon cycling (Malhi et al. 2002). Over the last few decades, estimation of above-ground biomass has received special attention to evaluate significance of forests in carbon sequestration and CO₂ emission vital to address global warming (Kumar and Mutanga 2017). Accurate, timely and reliable information on forest biomass and AGB mapping has become an important task for many purposes

such as sustainable forest management (Shao and Zhang 2016; Maack et al. 2015), reporting of carbon stocks and changes (Kelsey and Neff 2014; Fayad et al. 2016; Clerici et al. 2016), climate change modelling studies (Zhu and Liu 2015; Galidaki et al. 2017) and management decision making (Persson 2016). Above-ground biomass estimation capitulates fundamental information to develop inventories for sustainable forest management (Pandit et al. 2018; Chung et al. 2009) and provides basis for most international negotiations in carbon trading schemes (Kumar and Mutanga 2017). It also enables professionals to monitor ecosystem responses and contributions towards global carbon cycling and climate change along with carbon accounting (Lu 2006; Güneralp et al. 2014; Gara et al. 2014; Chinembiri et al. 2013) leading to precise decision making to boost conservation efforts based on appropriate planning (Pandit et al. 2018). The measurement of forest AGB (which includes all vegetation above the ground) is usually made in metric tons of dry matter per hectare or in metric tons of carbon per hectare (Rodríguez-Veiga et al. 2017).

Sustainable forest management demands non-destructive, accurate and cost efficient biomass estimation (Arevalo et al. 2007). Though traditional methods of forest biomass inventories are considered to be more accurate but their adoption becomes impractical since they are time consuming, destructive, labor intensive, difficult and costly (Zhu and Liu 2015; Persson 2016; Meng et al. 2016; Lu et al. 2016). Moreover, it is commonly observed that estimate of biomass and carbon stock which solely based on forest inventory data have attributional, spatial and temporal gaps. Remote sensing can help deal with this challenge and these gaps can be filled to have more accurate estimates. Remote sensing information, that is captured at local, regional as well as global scales through different sources (optical and microwave), can be related to biomass in different ways (Kumar et al. 2015) and by virtue of its large spatial and temporal coverage it becomes possible to carry out forest biomass estimation at multiple scales (Du et al. 2014). It has been widely used for forest biomass estimation and the estimation of aboveground biomass (AGB) in particular (Gao et al. 2018).

AGB cannot be measured directly from space,

instead, the information derived from remotely sensed data is correlated to field based biomass estimates (Zhu and Liu 2015; Lu et al. 2016). Using a combination of field-based measurements and remote sensing, the estimation of common forest attributes (biomass, height, stem diameter, stem volume, and base area) is evident from many studies (Persson 2016). Spectrally derived parameters from sensor reflectance (bands) combined with field based measurements can enhance accuracy of biomass prediction (Dong et al. 2003). Field based measurements are used for development and validation of AGB predictive modelling thus they become an important source in remote sensing based methodologies for calibrating models and verifying results (Galidaki et al. 2017).

A variety of empirical modeling methods that include both parametric and non-parametric approaches are used to link remotely sensed data and AGB but so far none of them has proved to be a single best method. There are many factors like scale, sample size, study area terrain and results evaluation techniques that affect the performance of these methods (Zhu and Liu 2015). Among parametric methods, regression analysis has been a commonly used approach. This method of AGB estimation, which is less complex and yields relatively good results has been widely used in tropical, subtropical, and temperate forest ecosystems (Gao et al. 2018). Particularly, stepwise regression is used in regression based AGB modelling since it can automatically identify the predictor variables and in general, the data sets used for AGB modelling consists of spectral bands, vegetation indices, image transforms (like PCA) and image textures (Chen et al. 2019b). Regression based models take spectral bands, vegetation indices, and textural images as independent variables with biomass as dependent variable (Lu et al. 2016). Usually, medium resolution satellite data (e.g LANDSAT, ASTER, SPOT) with spatial resolution of 10-100 m (Kumar et al. 2015) is employed for biomass estimation at local scales (Avitabile et al. 2012). A number of studies (for instance (Zhu and Liu 2015; Wani et al. 2015; Vicharnakorn et al. 2014; Lopez-Serrano et al. 2015; Fernández-Manso et al. 2014; Chen et al. 2019b) carried out regression based AGB modelling using medium resolution remote sensing data that involved different combinations of a variety of

satellite derived parameters and field inventory data. The hyperspectral remote sensing technologies have some limitations (Mathieu et al. 2013) which include increased image costs, data volume, data redundancy, and data processing costs (Plaza et al. 2009; Lefsky et al. 2001; Govender et al. 2007; Bajcsy and Groves 2004). This constraint has shifted the focus towards the use of Landsat and other optical sensors such as Sen-tinel-2 which offer free and readily available broadband image data (Sibanda et al. 2015) that allow timely AGB and carbon accounting from local to regional scale (Laurin et al. 2018; Hall et al. 2011; Gibbs et al. 2007). Although Landsat images have widely been used for AGB estimation due to freely-available long archive but users have encountered data saturation problem because of low level of spatial resolution leading to under-estimation of biomass. For example, Kasischke et al. (2014) reported variations in biomass and vegetation indices attributable to saturation of spectral indices at higher biomass values. Similarly, Steininger (2000) has also confirmed saturation of spectral values at approximately 150 t/ha while some studies completely disapproved the use of multi-spectral data for biochemical properties and plant biomass (Broge and Mortensen 2002) due to insensitivity of multispectral data with low spectral resolution towards differences in plant characteristics. The importance of aboveground biomass (AGB) estimation using high spatial resolution satellite data has been underlined for monitoring of carbon stocks and variability and trends of terrestrial carbon fluxes (Liu et al. 2019).

Sentinel 2 is a polar orbiting imaging mission of European Space Agency (ESA) that was launched on 23rd June 2015. It is characterized by wide swath, multi-spectral imaging capability and high spatial as well as temporal resolutions. As compared to the current generation of Landsat sensors it provides imageries with significantly improved spatial, spectral and temporal resolutions (Castro Gomez 2017). The mission comprises of two satellites (2A & 2B) that are equipped with multi-spectral instrument (MSI). It offers high potential for a wide range of applications like forestry, agriculture, land management, disaster management and humanitarian relief operations (Aschbacher and Milagro-Pérez 2012). It captures data in 13 spectral

bands (ranging from visible to near infrared to shortwave infra-red) which makes it a potential source for mapping of various vegetation characteristics. Across the given thirteen spectral bands, imaging is carried out at 10 m (four bands), 20 m (six bands) and 60 m (three bands) spatial resolutions (Pandit et al. 2018). The Sentinel-2 Mission guarantees continued availability of the Sentinel 2 data for future (Rodríguez-Veiga et al. 2017).

Though various studies have reported the usefulness of Sentinel-2 data with major focus on estimating and predicting forest stock volume (CAO et al. 2018), burn severity (Fernández-Manso et al. 2016), forest biophysical variables (Majasalmi and Rautiainen 2016), evaluation of forest fire (Navarro et al. 2017), assessment of range land quality (Ramoelo et al. 2015) and forest canopy (Godinho et al. 2018) using red-edge bands/spectral indices and textures, only a few studies have attempted for AGB estimation using an integration of field plots observations and Sentinel 2 MSI data either alone (Pham et al. 2018; Pham et al. 2020; Pandit et al. 2019, 2018; Nuthammachot et al. 2018; Chen et al. 2019b) or in combination with a Sentinel 1 SAR (Nuthammachot et al. 2020; Liu et al. 2019; Chen et al. 2019a; Castillo et al. 2017; Agata et al. 2018) in different regions and forest types and have reported promising results. Recently, using Sentinel 2 data and machine learning technique, Pandit et al. (2018) and Pandit et al. (2019) have established AGB estimation model in subtropical forest where the study area is characterized by flat topography and the forest cover has a continuous stretch with broad leaved as dominating tree species. However, potential of Sentinel-2 data for AGB estimation in a terrestrial ecosystem is yet to be reported from within Pakistan where the review of pertinent literature reveals that there is not even a single study available regarding AGB estimation employing optical satellite data. Therefore, this study is vital to fill knowledge based gap while its utility is well demanded to modernize conventional inventories for sustainable forest management. Reliable provision of high quality Sentinel 2 satellite data will not only facilitate forest biomass/carbon predictive modelling in future but it will also enable consistent monitoring of historical carbon stock changes which is a

prerequisite for sustainable forest management. This study was aimed to assess the application of Sentinel-2 multiband satellite data in conjunction with field observations for AGB estimation in a fragmented subtropical pine forest of the Pakistan administered state of Azad Jammu and Kashmir (AJK).

1 Materials and Methods

The dataset used for AGB prediction modelling involved field measured AGB from sample plots, various spectral and textural variables derived from Sentinel 2A satellite image and the topographic features extracted from ALOS PALSAR Digital Elevation Model (DEM). This section describes the study area, steps taken for preparation of required dataset and statistical analysis adopted for AGB/carbon estimation modelling.

1.1 Study area

The study area is located between $33^{\circ}35'19''$ - $33^{\circ}50'14''$ N and $73^{\circ}35'45''$ - $73^{\circ}53'45''$ E (Figure 1) in Sudhnuti district of Pakistan administered state of Azad Jammu & Kashmir and covers a stretch of 471 km². The tract is mountainous characterized by

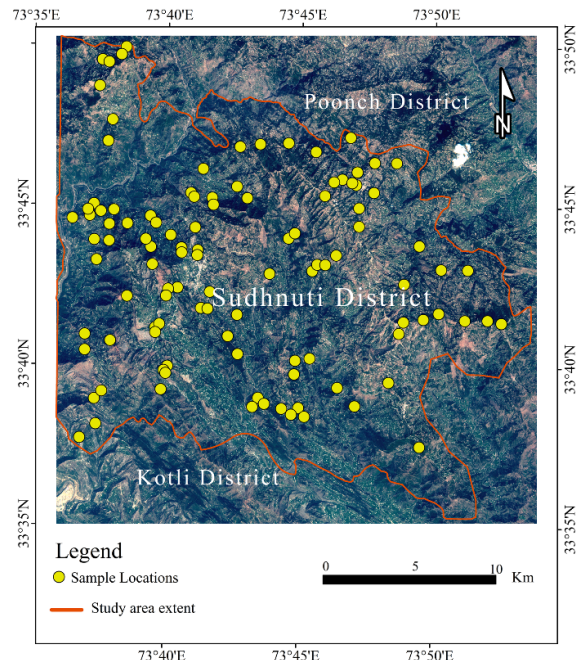


Figure 1 Map of the study area with sample points distribution.

rugged topography where elevation ranges from 385 m asl to 2121 m asl with varying degree of slope. Mean annual minimum and maximum temperature is 11°C and 25°C, respectively. June-July are the hottest months and ascending from south to north the severity of temperature decreases with elevation. Average annual precipitation is 1432 mm, most of which is received as monsoon rains in summer with occasional showers and snowfall at high altitudes in winter. Natural vegetation of the area comprises of subtropical pine forest mainly dominated by Chir Pine (*Pinus roxburghii*) with a little mix of blue pine (*Pinus wallichiana*) towards upper limits (Siddiqui 1997). Chir pine (*Pinus roxburghii*) is native to Himalaya and it is also known as Himalayan long needle pine. It grows between 450 and 2300 m asl with its coverage mainly confined to the areas of heavy monsoon. In Himalaya, its distribution can be observed as pure forests over wide areas with a little mixture of broad leaved and other coniferous species (*Cedrus deodara* and *Pinus wallichiana*)

towards the upper limits (Sharma and Baduni 2000). It is an important natural resource of the state because it serves as a valuable carbon sink for sequestration of atmospheric carbon. The area is densely populated with major population scattered in rural areas within proximity of forested patches. These state-owned forests are managed by the Department of Forest, State of AJK, Pakistan.

1.2 Field data collection

A pilot survey of the study area was conducted to collect preliminary information required to determine a sample size for the study area. Based

on the mean carbon stock estimated through reconnaissance survey 108 number of sampling plots were calculated using equation 1 (Pearson et al. 2005).

$$n = \frac{(N \times s)^2}{\frac{N^2 \times E^2}{t^2} + N \times s^2} \quad (1)$$

where n = number of sample plots, E = allowable error (10%), t = statistical value at 95% significance level, s = standard deviation, N = area of the plot in hectares. Distribution of sample points across the study area is depicted through Figure 1.

Using Geographic Information System these plots were randomly distributed across the study area (Figure 1). Field observations were collected in January – April, 2017. The position of each circular plots (0.1 ha) was determined through a handheld Global Positioning System (GPS) and slope of the site was recorded by using a clinometer to adjust the plot area accordingly (Pearson et al. 2005). Within each sample plot, diameter at breast height (DBH) and tree height (H) of all trees having diameter >15 cm was recorded using tree caliper

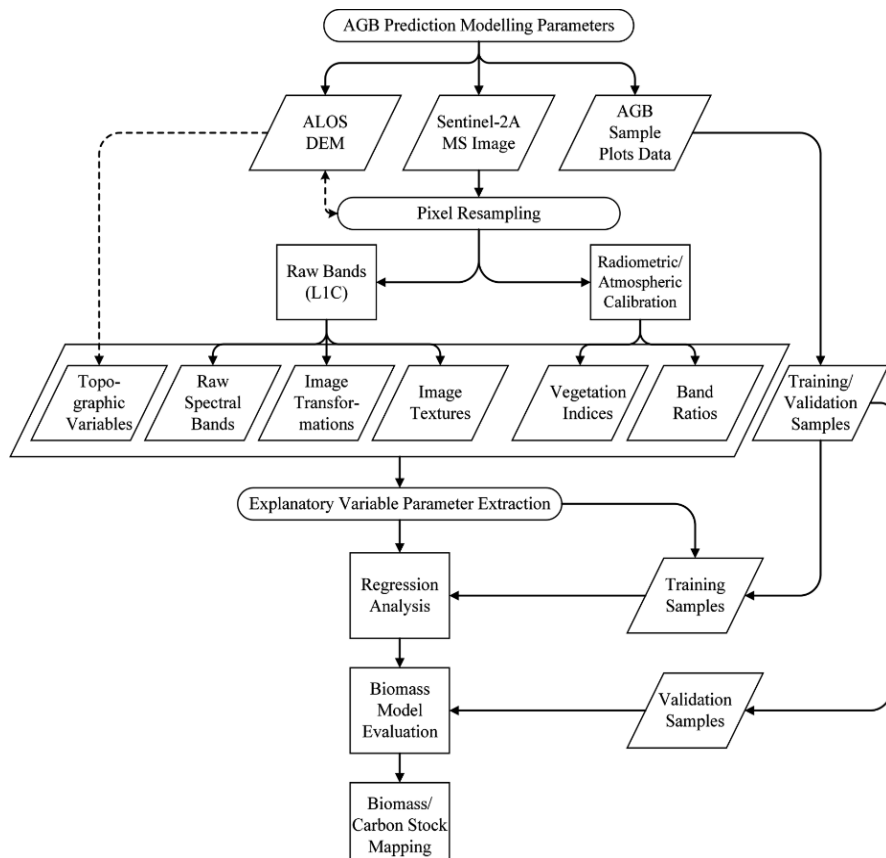


Figure 2 Process flow diagram of above ground biomass (AGB)/carbon mapping of the study area.

and Abney level respectively.

1.3 Satellite data collection

The Multi-spectral moderate resolution satellite data (S2MSI1C image) acquired by the Sentinel-2A satellite (S2A_MSIL1C_20170327T054631_N0204_R048_T43SCT_20170327T055732) on March 27, 2017 was downloaded from Sentinels Scientific Data Hub (<https://scihub.copernicus.eu/>). The Digital Elevation Model as part of high resolution terrain corrected ALOS dataset (Granule: ALPSRP264850660) corresponding to the study area was downloaded from “Alaska Satellite Facility’s Data Portal (<https://vertex.daac.asf.alaska.edu/>)”. Both of these products are available free of charge from referred sources.

1.4 Calculation of AGB

The Pakistan Forest Institute (PFI), Peshawar has recently developed biomass/carbon tables for major tree species of Khyber Pakhtunkwa (KPK) and Gilgit Baltistan (GB) provinces. As the coniferous vegetation of these provinces is similar to the study, therefore, above ground biomass (AGB) for inventoried tree species was calculated by retrieving local allometric equations from technical reports of PFI. A conversion factor of 0.5 ([Basuki et al. 2009](#)) was used to quantify the carbon held by biomass. Flow of information for carbon mapping is shown in [Figure 2](#).

1.5 Extraction of satellite image variables

The Sentinel 2A images with varying spatial resolutions (10 m – 60 m) have wide spectral coverage (imagery is captured in 13 spectral bands over VNIR and SWIR range of electromagnetic Spectrum). The bands configuration of Sentinel-2A MSI ([Fernández-Manso et al. 2016](#)) is provided in [Table 1](#).

Sentinel-2A image product (S2MSI1C) has processing Level 1C which includes radiometric and geometric corrections with sub-pixel accuracy ([ESA 2015](#)). Only the spectral bands with 10 m and 20 m spatial resolution were used and three spectral bands with 60 m spatial resolution were not included in the analysis. Keeping in view the

varying spatial resolution of Sentinel-2 spectral bands, spatial data resampling was applied to obtain uniform pixel size of 20 m for all selected multispectral bands. The image data was calibrated to ground reflectance utilizing the ATCOR module of PCI Geomatica 2017 (Trial Version). Using medium resolution satellite data many studies have attempted to investigate the relationship between AGB and satellite spectral values like digital numbers, radiance, reflectance and vegetation indices ([Tian et al. 2012](#)). The rescaled surface reflectance data was used for derivation of various spectral variables (such as vegetation indices, band ratios and image transforms) and a number of image textures to establish AGB estimation model using AGB measurements collected from sample plots ([Table 2](#)).

As far as the biomass estimation using remote sensing data is concerned, undoubtedly remote sensing techniques have many advantages over conventional methods. However, heterogeneous forest stand structures and spectral saturation problem of remote sensing data may reduce the accuracies of biomass estimation models which are based solely on spectral information ([Li et al. 2008](#)). Texture reflects the roughness of surfaces and it provides useful information on forest structural and geometric properties ([De Grandi et al. 2009](#)). Synergetic use of spectral responses and textures in combination can be helpful to establish more accurate biomass estimation models than using either spectral responses or textures alone ([Lu 2005](#)). Many techniques are used for extraction of textures from remote sensing images where gray level co-occurrence matrix (GLCM)-based texture measures are used commonly ([Lu et al. 2016](#)). It is a statistical method that is employed with moving

Table 1 Bands configuration of Sentinel-2A multi-spectral instrument (MSI)

Acronym	Band	Center wavelength (nm)	Spatial resolution (m)
2	Blue	490	10
3	Green	560	10
4	Red	665	10
5	Red-Edge 1	705	20
6	Red-Edge 2	740	20
7	Red-Edge 3	783	20
8	NIR	842	10
8a	NIR Narrow	865	20
11	SW1	1610	20
12	SW2	2190	20

widows of varying sizes on different spectral bands for extraction of textural information from all types of remotely sensed images (Cutler et al. 2012). There are a number of studies that have used GLCM based textural features for forest biomass estimation modeling with medium resolution (10–30 m) satellite data (Pandit et al. 2019; Nuthammachot et al. 2020; Lopez-Serrano et al. 2015; Kelsey and Neff 2014; Gao et al. 2018; Chen

et al. 2019b; Chen et al. 2018). As the combination of image based spectral and textural information improves the biomass estimation performance than using spectral responses or textural features alone (Lu 2005), therefore textural features which are commonly used in forest biomass estimation modelling (mean standard deviation and GLCM based variance, inverse distance moment, contrast, correlation, entropy and angular second moment)

Table 2 Set of different spectral and textural parameters used in stepwise regression based spectral modeling for mapping of above ground biomass (AGB)

Variables	Equations/Description	Reference
Spectral Bands	$B2, B3, B4, B5, B6, B7, B8, B8a, B11, B12$	
Band Ratios		
Ratio 1	$B8/B4$	
Ratio 2	$B8/B8a$	
Ratio 3	$B8a/B8$	
Ratio 4	$B6/B5$	
Ratio 5	$B7/B5$	
Ratio 6	$B4/B11$	
Ratio 7	$B4/B12$	
Vegetation Indices		
Normalized Difference Vegetation Index (NDVI)	$\frac{(B8 - B4)}{(B8 + B4)}$	Rousel et al. 1973
Enhanced Vegetation Index (EVI)	$2.5 \times \frac{(B8 - B4)}{(B8 + 0.6 \times B4 - 7.5 \times B2 + 1)}$	Huete et al. 1999
Difference Vegetation Index (DVI)	$(B8 - B4)$	Tucker 1979
Soil Adjusted Vegetation Index (SAVI)	$\frac{(B8 - B4)}{(B8 + B4 + 0.5)} \times (1 + 0.5)$	Huete 1988
Global environmental monitoring index (GEMI)	$n(1 - 0.25n) \frac{B4 - 0.125}{(1 - B4)} ; n = 2 \times (B8^2 - B4^2) + 1.5 \times B8 + 0.5 \times B4$	Pinty and Verstraete 1992
Image Transforms		
Blue-Green-Red (VIS234)	$(B2 + B3 + B4)$	
Albedo	$(B2 + B3 + B4 + B5 + B6 + B7 + B8 + B8a + B11 + B12)$	As used by (Lu et al. 2004) for Landsat
Red-Edge Spectral Indices		
Simple Ratio	$(B8/B4)$	
Normalized Difference Vegetation Index red-edge 1 (NDVIRE1)	$\frac{(B8 - B5)}{(B8 + B5)}$	
Normalized Difference Vegetation Index red-edge 1 narrow (NDVIRE1n)	$\frac{(B8a - B5)}{(B8a + B5)}$	
Normalized Difference Vegetation Index red-edge 2 (NDVIRE2)	$\frac{(B8 - B6)}{(B8 + B6)}$	
Normalized Difference Vegetation Index red-edge 2 narrow (NDVIRE2n)	$\frac{(B8a - B6)}{(B8a + B6)}$	
Normalized Difference Vegetation Index red-edge 3 (NDVIRE3)	$\frac{(B8 - B7)}{(B8 + B7)}$	
Normalized Difference Vegetation Index red-edge 3 narrow (NDVIRE3n)	$\frac{(B8a - B7)}{(B8a + B7)}$	
Red Edge Inflection Point (REIP)	$70 + 40 \times \frac{\frac{B4 + B7}{2} - B5}{(B6 - B5)}$	Guyot et al. 1988
Image Textures		
First order statistical Textures	Mean, Standard Deviation, Variance, Entropy	
Second order GLCM based Textures	ASM, Contrast, Correlation, IDM	Haralick et al. 1973

were also included in AGB estimation modelling. Since topography influences the spatial distribution of vegetation (Li et al. 2008), therefore some biomass estimation studies have included this information as well (Wijaya et al. 2010; Vicharnakorn et al. 2014; Li et al. 2008; Chen et al. 2019b). The topographic variables viz. elevation and slope derived from ALOS Digital Elevation Model (DEM) were also included in the array of predictive variables. Prior to extraction of topographic variables, the DEM was resampled to 20 m pixel size to maintain consistency with spectral and textural attributes resulted from image data.

The Sentinel-2A derived variables used in this study are shown in Table 2. The derived spectral parameters include simple ratios, vegetation indices and image transforms whereas mean, standard deviation, variance, entropy, angular second moment (ASM), correlation, contrast and inverse distance moment (IDM) are the image textures which were calculated for all spectral bands using window sizes of 3×3, 5×5, 7×7, 9×9, 11×11, 13×13, 15×15, 17×17 and 19×19. Out of 108 sample points, 54 points were randomly separated for AGB predictive modelling whereas half of the sample points were used for model validation.

In order to avoid the mismatch between the spatial extent covered by field plot and the pixel of remote sensing image and to compensate the GPS error, an average of 3×3 was used to extract values of selected spectral, textural and topographic variables for AGB predictive modelling. The multiple stepwise regression analysis was applied to determine significant ($p<0.05$) predictive variables. In stepwise regression method of AGB modelling, the variables are introduced one by one to identify the significant variables and an original explanatory variable is deleted when it stands no longer significant with the introduction of a new explanatory variable and this process continues till the most significant variables that have no serious multicollinearity problem are identified and selected for the regression equation (Chen et al. 2019b). Pearson's R , R^2 and adjusted R^2 were used to evaluate the model performance. Reliability of the model was based on multicollinearity of variables where only the models including variables with tolerance value > 0.1 and VIF value < 10 were taken into consideration (Nuthammachot

et al. 2018; Eckert 2012). Figure 2 illustrates the steps followed for AGB predictive modelling.

Root mean square error (RMSE) between predicted and observed AGB values was calculated using the Eq. 2. Correlations among different independent variables and the dependent variable were also examined.

$$\text{RMSE} = \sqrt{\frac{\sum_{i=1}^n (\bar{y} - y)^2}{n}} \quad (2)$$

where \bar{y} and y refer to the predicted and corresponding AGB at the sample plot i .

The following combinations of parameters were tried in step wise regression method for AGB predictive modelling.

- A. Spectral indices, spectral bands & band ratios;
- B. Spectral indices, band transforms & DEM derived topographic features;
- C. Red edge indices, red edge spectral bands and red edge band ratios;
- D. Red edge indices, spectral bands and band ratios with topographic features;
- E. A, B, C & D together;
- F. First order textures;
- G. Second order textures;
- H. F & G together;
- I. F&G with topographic features;
- J. A, F & G with topographic features;
- K. A, B, F & G with Topographic features;
- L. All A-D, F & G.

2 Results

The mean AGB value calculated from sample plots was 144.5 t/ha and the coressponding average biomass carbon stock value was worked out as 72.25 t/ha for the study area. The stepwise linear regression yielded a range of AGB prediction models but only the best performance models having adjutsed $R^2 > 0.5$ and predictor variables with $p < 0.05$ were chosen (Table 3). Model 1 with highest R (0.86), R^2 (0.74) and adjusted R^2 (0.72) and lowest RMSE value (33 t/ha) was selected for AGB mapping. A biomass map of the study area was generated using Eq.3 that is based on model 1 (Table 3) and a multiplicative factor of 0.5 (Wani et al. 2015) was used to develop a carbon map of the study area (Figure 3). A scatter plot (Figure 4) shows correlation between the predicted and observed AGB for the generated models (1-4). In case of model 1 a strong coefficient of determination ($R^2=0.74$) indicates that this model has the ability to explain 74% of AGB variability. Corelations of AGB against different Sentinel-2A

derived spectral and textural features are furnished in Table 4.

$$AGB = -857.775 + \left\{ (-35.242 \times B6 \text{ Mean } 19 \times 19) + \left(1523.112 \times \frac{B8}{B8a} \right) + (-32.349 \times B12 \text{ SD } 15 \times 15) + (18.209 \times B11 \text{ Mean } 15 \times 15) + (-4.692 \times B12 \text{ Variance } 13 \times 13) \right\} \quad (3)$$

3 Discussion

Our field inventory based average AGB and corresponding carbon stock values are 144.5 t/ha and 72.25 t/ha, respectively. However, forest C stock varies according to geographic location, plant species and age of plant stand (Van Noordwijk et al. 1997; Harmon and Hua 1991), which makes it difficult to draw a comparative analysis with other geographical and regional findings. Nevertheless, our estimates are consistent with some studies conducted in the Himalayan region. For instance, Sharma et al. (2010) have reported AGB estimates of 126.23 ± 12.81 and 239.86 ± 46.09 for Siwalik *Pinus roxburghii* and Himalayan *Pinus roxburghii*, respectively. Rana et al. (1988) reported above ground biomass value of 163 t/ha for central Himalayan Chir pine (*Pinus roxburghii*) forests whereas the reported AGB range for Kuman *Pinus roxburghii*, and Pauri Garhwal *Pinus roxburghii*, is 163-232.3 t/ha and 126.2-239.9 t/ha, respectively (Gairola et al. 2011). In Subtropicalforests of Pakistan, Nizami (2012) has determined the average above ground biomass (excluding root biomass) for *Pinus roxburghii* as 161 t/ha - 198 t/ha and findings of Shaheen et al. 2016 revealed average biomass value of 191.8 t/ha for subtropical forest types of Kashmir Himalaya. These small differences observed in biomass estimates of *Pinus roxburghii* may be attributed to difference in altitudinal ranges (Gairola et al. 2011), aspects (Sharma and Baduni 2000), forest type (Sharma et al. 2010) and site quality (Gosain 2016) . Besides, poor management systems, population pressure, un-planned infrastructural developments and high grazing pressure may also lead to variations in biomass recorded at different locations.

AGB estimation modelling based on field measured AGB and Sentinel 2 derived spectral and

Table 3 Stepwise linear regression models using field observations and Sentinel-2A optical data for above ground biomass (AGB) estimation

No.	Parameters	Coe.	R	R ²	R ² adj
1	Constant	-857.775			
	(i). B6 Mean (19×19)	-35.242			
	(ii). B8/B8a	1523.112	0.86	0.74	0.72
	(iii).B12 SD (15×15)	-32.349			
	(iv).B11 Mean (15×15)	18.209			
2	(v). B12 Variance (13×13)	-4.692			
	Constant	-949.659			
	(i). B6 Mean (19×19)	-34.536			
	(ii). B8/B8a	1611.555	0.86	0.74	0.71
	(iii).B12 SD (15×15)	-46.983			
3	(iv).B11 Mean (15×15)	20.798			
	(v). B4 Contrast (17×17)	-13.441			
	Constant	-891.308			
	(i). B6 Mean (19×19)	-34.816			
	(ii). B8/B8a	1581.988	0.84	0.71	0.69
4	(iii).B12 SD (15×15)	-46.032			
	(iv). B11 Mean (15×15)	16.416			
	Constant	-815.210			
	(i). B6 Mean (19×19)	-18.897			
	(ii). B8/B8a	1446.968	0.78	0.61	0.59
	(iii).B12 SD (15×15)	-29.123			

Note: No.= Model No.; SD = Std. Deviation; Coe.=Coefficients; R² adj= R² adjusted; B12, B11,B8, B8a and B6 are the spectral bands of Sentinel 2A imagery; 13×13, 15×15, 17×17 and 19×19 refers to the window size used for calculation of image textures.

textural variables have shown varying degree of success (Pandit et al. 2019; Chen et al. 2019b; Chen et al. 2019a; Chen et al. 2018). However, review of pertinent literature reveals that so far only few studies have attempted to evaluate the performance of Sentinel-2 for AGB estimation modelling through linear regression approach. For example, Nuthammachot et al. (2018) examined the suitability of Sentinel-2 imagery for AGB modelling in Indonesian tropical forest using field data and different vegetation indices. In this study, only spectral vegetation indices were used and an AGB prediction model was established through stepwise linear regression method. The study found a strong correlation ($R = 0.89$; $R^2 = 0.79$) between AGB and correlation ($R = 0.89$; $R^2 = 0.79$) between AGB and normalized difference index (NDI) with RMSE value of 27 Mg/ha. In another case, Castillo et al. (2017) reported that a combination of Sentinel-2 derived red and red edge bands and elevation data proved best for AGB prediction in mangrove forests of Philippines. Based on different combinations of Sentinel 2A spectral and textural variables along with ALOS

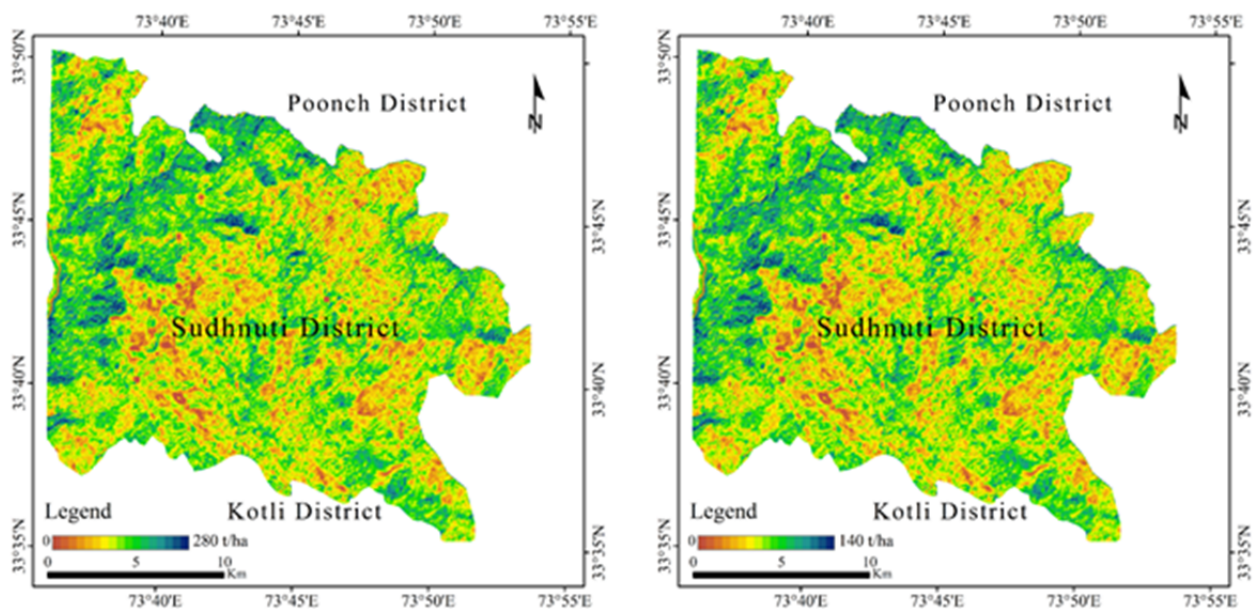


Figure 3 Biomass (left) and carbon (right) maps of the study area generated from the established model 1.

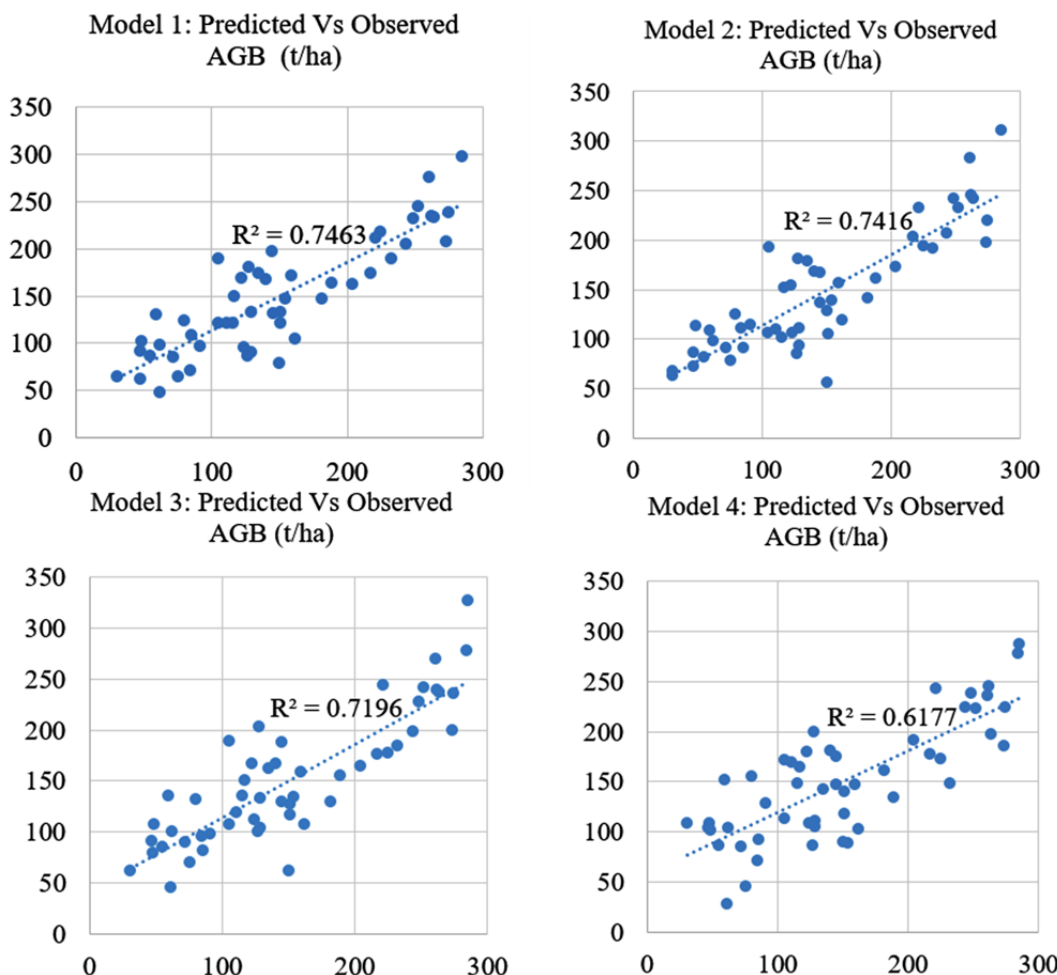


Figure 4 A scatterplot showing the relationship between measured above ground biomass (AGB) and the modeled above ground biomass (AGB) by using Model 1, Model 2, Model 3 and Model 4, respectively.

derived topographic features, the step wise linear regression method generated models with varying performance. Out of them, four models with best performance (adjusted $R^2 \geq 0.50$ at $P < 0.05$) are furnished in Table 3. In our study spectral features alone yielded an AGB prediction model ($R=0.68$, $R^2=0.47$, adjusted $R^2=0.42$) that embodied band 7 (red edge-3), band 8 (NIR), a ratio image (band 8/band8a) and a ratio image (b4/b12) as predictor variables. But model performance was poor because of strong intercorrelation among the bands. Profound multicollinearity problem was also indicated by Nichol and Sarker (2011) while conducting AGB estimation modeling in subtropical forest of Hong Kong where this problem was encountered in stepwise regression based AGB estimation model due to strong correlation among AVNIR-2 and SPOT-5 derived simple spectral bands and band ratios. Spectral bands of medium resolution satellite images have shown significant contribution in AGB prediction models developed through multiple linear regression method in different forest types and regions. Simple spectral bands of Sentinel-2, Landsat TM, ASTER and SPOT-5 images performed notably in AGB prediction models established for mangrove forest in Philippines (Castillo et al. 2017), pine forest in Turkey (Günlü et al. 2014), tundra forest in Siberia (Fuchs et al. 2009) and cold arid forest in China (Tian et al. 2012) respectively. Similarly, significant contribution of band ratios was observed in AGB estimation models developed by Vicharnakorn et al. (2014) for different vegetation covers in Lao PDR ($R=0.72$ and $R=0.93$) and Zheng et al. (2004) for hardwood and pine forest of Wisconsin, USA ($R^2=0.82$). In this study none of the normalized vegetation indices, band transforms and topographic features participated in established AGB estimation models. Though spectral vegetation indices derived from medium resolution satellite image played important role in biomass prediction models performed in different forest ecosystems (Wani et al. 2015; Nuthammachot et al. 2018; Heiskanen 2006; Gasparri et al. 2010), yet few studies (Wijaya

Table 4 Correlation among above ground biomass (AGB) and different Sentinel 2A derived spectral and textural variables

Parameter	R	Parameter	R
B3 mean (19×19)	0.436**	B7 mean (15×15)	0.625**
B5 mean (19×19)	0.530**	B8 mean (15×15)	0.582**
B6 mean (19×19)	0.647***	B8a mean (15×15)	0.612**
B7 mean (19×19)	0.646**	B11 mean (15×15)	0.450**
B8 mean (19×19)	0.603**	B12 mean (15×15)	0.413**
B8a mean (19×19)	0.635**	B2SD (15×15)	0.480**
B11 mean (19×19)	0.478**	B3SD (15×15)	0.459**
B12 mean (19×19)	0.441**	B4 SD (15×15)	0.490**
B2SD (19×19)	0.460**	B5 SD (15×15)	0.413**
B3SD (19×19)	0.423**	B11 SD (15×15)	0.424*
B4 SD (19×19)	0.474**	B12 SD (15×15)	0.465**
B12 SD (19×19)	0.408**	B2 Contrast (15×15)	0.404*
B2 Contrast (19×19)	0.404*	B4 Contrast (15×15)	0.427**
B4 Contrast (19×19)	0.427**	B12 Contrast (15×15)	0.436**
B12 Contrast (19×19)	0.436**	B12 IDM (15×15)	0.403**
B12 IDM (19×19)	0.403**	B12 IDM (15×15)	0.401**
B3 mean (17×17)	0.431**	B4 Variance (15×15)	0.426**
B4 mean (17×17)	0.470**	B11 Variance (15×15)	0.408**
B5 mean (17×17)	0.517**	B12 Variance (15×15)	0.423**
B6 mean (17×17)	0.635**	B4 Correlation (15×15)	0.418**
B7 mean (17×17)	0.636**	B5 mean (13×13)	0.487**
B8 mean (17×17)	0.595**	B6 mean (13×13)	0.612**
B8a mean (17×17)	0.624**	B7 mean (13×13)	0.615**
B11 mean (17×17)	0.465**	B8 mean (13×13)	0.572**
B12 mean (17×17)	0.427**	B8a mean (13×13)	0.602**
B2SD (17×17)	0.482**	B11 mean (13×13)	0.437**
B3SD (17×17)	0.451**	B12 mean (13×13)	0.402**
B4 SD (17×17)	0.491**	B2 SD (13×13)	0.452**
B12 SD (17×17)	0.432**	B3 SD (13×13)	0.426**
B3 Correlation (17×17)	0.418**	B4 SD (13×13)	0.459**
B4 Contrast (17×17)	0.427**	B5 SD (13×13)	0.429**
B12 Contrast (17×17)	0.426**	B11SD (13×13)	0.448**
B12 IDM (17×17)	0.455**	B12 SD (13×13)	0.485**
B2 Variance (17×17)	0.421**	B12 Contrast (13×13)	0.420**
B3 Variance (17×17)	0.414**	B11 Variance (13×13)	0.506**
B4 Variance (17×17)	0.438**	B12 Variance (13×13)	0.503**
B3 mean (15×15)	0.423**	Red Edge 2	0.486**
B5 mean (15×15)	0.499**	Red Edge 3	0.490**
B6 mean (15×15)	0.624**	Linear combination of Red edge bands	0.468**
B2 Correlation (13×13)	0.453**	B8	0.417**
B3 Correlation (13×13)	0.456**	B8a	0.475**
B2 Entropy (13×13)	0.465**	B5 Entropy (13×13)	0.447**
B3 Entropy (13×13)	0.413**	B11 Entropy (13×13)	0.434**

Note: *Correlations are significant ($P < 0.05$). **Correlations are significant ($P < 0.01$). 13×13, 15×15, 17×17 and 19×19 refers to the window size used for calculation of image textures.

SD= Standard Deviation; IDM= Inverse Distance Moment.

et al. 2010; Kumar and Ghose 2017; Fuchs et al. 2009; Foody et al. 2003) found no significant contribution of spectral vegetation indices in AGB modelling performance. This may be attributed to optical sensor data saturation problems that may arise in sites of high biomass density (Steininger 2000; Lu et al. 2016; Cohen and Spies 1992). It is

believed that texture analysis technique may improve biomass estimation in forest regions where spectral vegetation indices can saturate because it allows to identify the most suitable texture parameters to predict biomass through adjustment of window size (Kelsey and Neff 2014). All the model combinations demonstrated contribution from first order texture measures i.e mean and standard deviation. None of the normalized vegetation indices, band transforms and topographic features participated in established AGB estimation models. In prediction model 1 ([Table 3](#)) mean of band 6 (19×19), simple ratio of band 8 and band 8a, standard deviation of band 12 (15×15), mean of band 11 (15×15) and variance of band 12 (13×13) have provided the best combination for AGB predictive modelling in the study area characterized by fragmented forest landscape and mountainous topography.

Inclusion of textures in step-wise linear regression remarkably improved the prediction models. Potential of texture variables derived from medium resolution images is evident from many AGB prediction studies ([Wijaya et al. 2010; Safari and Sohrabi 2016; Nichol and Sarker 2011; Lu and Batistella 2005; Lu 2005; Lopez-Serrano et al. 2015; Li et al. 2008; Goh et al. 2013; Fuchs et al. 2009](#)). [Dube and Mutanga \(2015\)](#) have confirmed that image textures can enhance AGB estimation performance when compared to simple spectral bands, band ratios and spectral vegetation indices. A marked contribution from first order texture measures i.e mean and standard deviation was observed in models that included both spectral and textural variables ([Table 3](#)). In prediction model 1 ([Table 3](#)) mean of band 6 (19×19), simple ratio of band 8 and band 8a, standard deviation of band 12 (15×15), mean of band 11 (15×15) and variance of band 12 (13×13) provided the best combination for AGB predictive modelling in the study area characterized by fragmented forest landscape and mountainous topography. In multiple regression based AGB prediction modelling many studies conducted in different forest ecosystems have shown contribution of mean, standard deviation, variance and contrast textural variables derived from medium resolution Landsat OLI ([Dube and Mutanga 2015](#)), ASTER ([Fuchs et al. 2009](#)), SPOT-5 ([Li et al. 2008; Goh et al. 2013](#)), AVNIR-2 ([Nichol and Sarker 2011](#)), Landsat TM ([Safari and](#)

[Sohrabi 2016; Lu 2005; Lopez-Serrano et al. 2015](#)) and Landsat 7 ETM+ ([Wijaya et al. 2010](#)) satellite images where the authors have reported R^2 (0.76), R^2_{adj} (0.45), R^2 (0.64 and 0.49), R^2 (0.78), R^2 (0.53, 0.58 and 0.77) and R^2 (0.54) for these models, respectively.

Texture is a very complex property that is greatly influenced by the selected window size, environmental conditions and the nature of the object under investigation ([Marceau et al. 1990; Franklin 2001; Franklin et al. 1996; Chen et al. 2004](#)). Textures vary with the images used and the nature of the landscape ([Kumar et al. 2015](#)). As the texture varies with landscape characteristics and the image used, selection of suitable texture variables for biomass estimation is a challenging job. Selection of appropriate image band and suitable window size becomes crucial for identification of most suitable texture variables ([Safari and Sohrabi 2016](#)). In our study, in order to determine the optimal window size, textures were calculated using different window sizes. It was observed that textures with window size below 13×13 did not make any difference either alone or in combination with spectral and topographic features. Mean and standard deviation from different window sizes (13×13, 15×15 and 19×19) played a significant role in model improvement and the textures calculated using windows above 19×19 didn't work because of smoothing effect. Size of window chosen for calculation of textures plays an important role in determining the appropriate texture variables because a small window is sensitive to fine scale variations whereas a large window captures large scale variations in pixel brightness. Therefore, a very small window may provide exaggerated information whereas a very large window size may not be able to identify the important variations in pixel brightness (Kelsey and Neff 2014). All models shown in [Table 3](#) have participation from first order image textures (mean and standard deviation). The importance of these simple statistical parameters has also been underlined by [Li et al. \(2008\)](#) which endorse that minority textural measures play a significantly effective and critical role in estimating forest biomass. Our AGB prediction models 1, 2, 3 & 4 which are mainly based on simple statistical parameters (mean and standard deviations) with one spectral feature (band ratio) explain 72%, 71%,

69% and 59% of field variability with RMSE values of 33 t/ha, 36 t/ha, 39 t/ha and 45 t/ha, respectively. Using field inventory points earlier reserved for model validation purpose a comparison was made between the field estimated biomass and texturally/spectrally modelled biomass and a reasonably good correlation ($R^2=0.58$) was observed between the two. From amongst the GLCM based image textures (contrast, correlation, ASM, IDM, entropy and variance), only variance of band 12 (13×13) and contrast of band 4 (17×17) have made contribution in AGB prediction modelling whereas the rest of the second order image textures did not participate in modelling process. Texture parameters derived from an image band or different bands can be effectively used for AGB estimation modelling performed through multiple linear regression because different texture algorithms and multiple window sizes enable to generate uncorrelated texture measures which helps in fulfilling the condition that AGB prediction models developed from multiple linear regression must be based on uncorrelated variables (Nichol and Sarker 2011).

The correlation between different satellites derived spectral and texture variables and field measured AGB is given in Table 4. Mean of bands 6, 7, 8 and 8a with window size 19×19 showed strong correlation with AGB ($R\geq0.60$ at 0.01 significance level). Similar level of correlation was observed between AGB and mean image textures of bands 6, 7 and 8a calculated with window size of 17×17 , 15×15 and 13×13 . Mean of band 5 (19×19 and 17×17), band 8 (17×17 , 15×15 and 13×13) and variance of band 11 (13×13), band 12 (13×13) also demonstrated a strong correlation with AGB ($R\geq0.50$ at $P<0.01$). A moderate correlation ($R\geq0.40$ at $P<0.01$) was observed between AGB and mean of bands 3, 11 & 12, standard deviation of band 12, contrast of bands 4 & 12 and IDM of band 12 with window size 19×19 . Similarly, mean of bands 3, 11 & 12, standard deviation of bands 2, 3, 4, & 12, contrast of bands 4 & 12, variance of bands 2, 3 & 4 with window size 17×17 and mean of bands 3, 5, 11 & 12, standard deviation of bands 2, 3, 4, 5, 11 & 12, contrast of bands 4 & 12, IDM of band 12, correlation of band 4, variance of bands 4, 11 & 12 with window size of 15×15 have presented a moderate correlation with inventory based AGB. Besides, mean of bands 3, 5, 11 & 12, standard

deviation of bands 2, 3, 4, 5, 11 & 12, contrast of band 12, correlation of bands 2 & 3, ASM of bands 2, 5 & 12, entropy of bands 2, 3, 5, 11 & 12, variance of bands 2, 3, 4 & 5 with window size 13×13 showed a moderate correlation with the field measured AGB. Apart from this, strong correlation was observed between AGB and different spectral and texture features at $P<0.05$. A number of studies (Wijaya et al. 2010; Lu and Batistella 2005; Goh et al. 2013) found strong correlation (Pearson correlation coefficients $R>0.5$) between mean image textures and AGB whereas few studies (Li et al. 2008; Fuchs et al. 2009) observed moderate correlation ($R<0.5$) between these parameters.

From spectral domain a moderate correlation was observed among AGB and linear combination of red edge bands and spectral bands 6, 7, 8 & 8a. Studies have reported different correlation strengths between image spectral bands and AGB. Heiskanen (2006) and Fuchs et al. (2009) found a strong correlation between ASTER image spectral bands and AGB. A similar nature of correlation was observed between Landsat TM (Lu et al. 2004), Landsat 7 ETM+ (Gasparri et al. 2010) and SPOT 5 (Li et al. 2008) image bands and AGB. Strong correlation between above-ground biomass and TM spectral band ratios was reported by Lu et al. (2004) whereas Fuchs et al. (2009) observed very weak correlation between ASTER derived simple band ratios and AGB. Correlation analysis also revealed a significant correlation among AGB and different spectral and texture features at $P<0.05$ (Table 4). Sentinel 2A satellite data provides a worthwhile opportunity to establish AGB predictive model for the area of interest with reasonable accuracy. Hopefully, the derived information will help the concerned resource managers towards protection, conservation and management efforts aimed at sustainable forest management eventually enabling to participate in climate change mitigation efforts being carried out through different internationally agreed mechanisms under UNFCCC. The growing apprehension that further increase in population would have profound negative impact on existing fragmented carbon sink of the study area with consequential imbalance in natural equilibrium, continuous monitoring of this valuable resource is deemed essential. The planned continuity of sentinel mission in future would enable recurrent and

efficient forest management activities with minimum involvement of time, effort and resources, especially needful for resource-stricken organizations.

4 Conclusion

In this study potential of Sentinel-2A satellite data was evaluated for biomass estimation of the study area. Multiple linear regression based AGB predictive modeling that involved a combination of satellite derived independent variables and field measured AGB proved to be a cost effective and reliable approach for biomass estimation in fragmented subtropical pine forest of the study area that is characterized by rugged topography. Our study confirms that Sentinel- 2A based image textures (mean, standard deviation and variance) along with a band ratio provide the best combination to establish AGB estimation model with ability to explain 72% of variation in AGB accentuating its strength and reasonability. In established AGB prediction model, mean texture variable contributed the most, followed by standard deviation and variance. These textures can be calculated quite conveniently from Sentinel 2 optical data which is available free of cost from

online sources. Considering statistical evaluation of the resulted AGB model, it can be safely concluded that high quality moderate resolution Sentinel-2A data, being a remarkable free of cost resource can be utilized for regional level estimation of AGB and carbon stocks to pursue sustainable forest management especially in a resource constraint mountainous terrain. Though Sentinel 2 derived texture measures have significantly contributed in AGB predictive modelling in the study area, care has to be taken while using textures for a selected forest because textures are greatly influenced by the forest stand structure and the image used. It is anticipated that synergetic use of Sentinel 1 and 2 utilizing approaches other than regression such as machine learning algorithms (random forest, artificial neural network and support vector machine) might improve the overall accuracy of AGB estimation.

Acknowledgement

We are grateful to the Department of Forests, State of AJK (Pakistan) for providing logistic support during field inventory. We would also like to express our gratitude to the reviewers for improving the manuscript with their thoughtful suggestions.

References

- Agata H, Aneta L, Dariusz Z, et al. (2018) Forest aboveground biomass estimation using a combination of Sentinel-1 and Sentinel-2 Data. In: IGARSS-IEEE International Geoscience and Remote Sensing Symposium, 2018. IEEE 9026-9029. <https://doi.org/10.1109/IGARSS.2018.8517965>
- Arevalo CB, Volk TA, Bevilacqua E, et al. (2007) Development and validation of aboveground biomass estimations for four *Salix* clones in central New York. *Biomass and Bioenergy* 31(1): 1-12. <https://doi.org/10.1016/j.biombioe.2006.06.012>
- Aschbacher J, Milagro-Pérez MP (2012) The European Earth monitoring (GMES) programme: Status and perspectives. *Remote Sensing of Environment* 120:3-8. <https://doi.org/10.1016/j.rse.2011.08.028>
- Avitabile V, Baccini A, Friedl MA, et al. (2012) Capabilities and limitations of Landsat and land cover data for aboveground woody biomass estimation of Uganda. *Remote Sensing of Environment* 117: 366-380. <https://doi.org/10.1016/j.rse.2011.10.012>
- Bajcsy P, Groves P (2004) Methodology for hyperspectral band selection. *Photogrammetric Engineering & Remote Sensing* 70(7): 793-802. <https://doi.org/10.14358/PERS.70.7.793>
- Basuki T, Van Laake P, Skidmore A, et al. (2009) Allometric equations for estimating the above-ground biomass in tropical lowland Dipterocarp forests. *Forest Ecology and Management* 257(8): 1684-1694. <https://doi.org/10.1016/j.foreco.2009.01.027>
- Broge NH, Mortensen JV (2002) Deriving green crop area index and canopy chlorophyll density of winter wheat from spectral reflectance data. *Remote Sensing of Environment* 81(1): 45-57. [https://doi.org/10.1016/S0034-4257\(01\)00332-7](https://doi.org/10.1016/S0034-4257(01)00332-7)
- Cao L, Peng D, Wang X (2018) Estimation of forest stock volume with spectral and textural information from the Sentinel-2A. *Journal of Northeast Forestry University* 46(9): 54-58.
- Castillo JAA, Apan AA, Maraseni TN, et al. (2017) Estimation and mapping of above-ground biomass of mangrove forests and their replacement land uses in the Philippines using Sentinel imagery. *ISPRS Journal of Photogrammetry and Remote Sensing* 134: 70-85. <https://doi.org/10.1016/j.isprsjprs.2017.10.016>
- Castro Gomez MG (2017) Joint use of Sentinel-1 and Sentinel-2 for land cover classification: A machine learning approach. Lund University GEM thesis series. <http://lup.lub.lu.se/student-papers/record/8915043>
- Chen D, Stow D, Gong P (2004) Examining the effect of spatial resolution and texture window size on classification accuracy: an urban environment case. *International Journal of Remote Sensing* 25(11): 2177-2192. <https://doi.org/10.1080/01431160310001618464>
- Chen L, Ren C, Zhang B, et al. (2018) Estimation of forest above-ground biomass by geographically weighted regression and machine learning with Sentinel imagery. *Forests* 9 (10): 582. <https://doi.org/10.3390/f9100582>
- Chen L, Wang Y, Ren C, et al. (2019a) Optimal combination of predictors and algorithms for forest above-ground biomass

- mapping from Sentinel and SRTM data. *Remote Sensing* 11(4): 414. <https://doi.org/10.3390/rs11040414>
- Chen Y, Li L, Lu D, et al. (2019b) Exploring Bamboo Forest Aboveground Biomass Estimation Using Sentinel-2 Data. *Remote Sens* 11 (1):7. <https://doi.org/10.3390/rs11010007>
- Cheng J, Lee X, Theng BK, et al. (2015) Biomass accumulation and carbon sequestration in an age-sequence of Zanthoxylum bungeanum plantations under the Grain for Green Program in karst regions, Guizhou province. *Agricultural and Forest Meteorology* 203: 88-95
<https://doi.org/10.1016/j.agrformet.2015.01.004>
- Chinembiri T, Bronsveld M, Rossiter D, et al. (2013) The precision of C stock estimation in the Ludhikola watershed using model-based and design-based approaches. *Natural Resources Research* 22(4): 297-309.
<https://doi.org/10.1007/s11053-013-9216-6>
- Chung SY, Yim JS, Cho HK, et al. (2009) Comparison of forest biomass estimation methods by combining satellite data and field data. *Proceedings Extending Forest Inventory and Monitoring*, 114.
- Clerici N, Rubiano K, Abd-Elrahman A, et al. (2016) Estimating aboveground biomass and carbon stocks in periurban Andean secondary forests using very high resolution imagery. *Forests* 7 (7): 138. <https://doi.org/10.3390/f7070138>
- Cohen WB, Spies TA (1992) Estimating structural attributes of Douglas-fir/western hemlock forest stands from Landsat and SPOT imagery. *Remote Sensing of Environment* 41 (1): 1-17.
[https://doi.org/10.1016/0034-4257\(92\)90056-P](https://doi.org/10.1016/0034-4257(92)90056-P)
- Cutler M, Boyd D, Foody G, et al. (2012) Estimating tropical forest biomass with a combination of SAR image texture and Landsat TM data: An assessment of predictions between regions. *ISPRS Journal of Photogrammetry and Remote Sensing* 70: 66-77.
<https://doi.org/10.1016/j.isprsjprs.2012.03.011>
- Dar JA, Sundarapandian S (2015) Variation of biomass and carbon pools with forest type in temperate forests of Kashmir Himalaya, India. *Environmental Monitoring and Assessment* 187(2): 55. <https://doi.org/10.1007/s10661-015-4299-7>
- De Grandi G, Lucas R, Kropacek J, et al. (2009) Analysis by wavelet frames of spatial statistics in PALSAR data for characterizing structural properties of forests. *IEEE Transactions on Geoscience and Remote Sensing* 47(2): 494-507. <https://doi.org/10.1109/TGRS.2008.2006183>
- Dong J, Kaufmann RK, Myneni RB, et al. (2003) Remote sensing estimates of boreal and temperate forest woody biomass: carbon pools, sources, and sinks. *Remote Sensing of Environment* 84(3): 393-410.
[https://doi.org/10.1016/S0034-4257\(02\)00130-X](https://doi.org/10.1016/S0034-4257(02)00130-X)
- Du L, Zhou T, Zou Z, et al. (2014) Mapping forest biomass using remote sensing and national forest inventory in China. *Forests* 5(6): 1267-1283. <https://doi.org/10.3390/f5061267>
- Dube T, Mutanga O (2015) Investigating the robustness of the new Landsat-8 Operational Land Imager derived texture metrics in estimating plantation forest aboveground biomass in resource constrained areas. *ISPRS Journal of Photogrammetry and Remote sensing* 108: 12-32.
<https://doi.org/10.1016/j.isprsjprs.2015.06.002>
- Eckert S (2012) Improved forest biomass and carbon estimations using texture measures from WorldView-2 satellite data. *Remote Sensing* 4(4): 810-829.
<https://doi.org/10.3390/rs4040810>
- ESA (2015) European Spatial Agency, 2015. Sentinel-2 user handbook ESA Standard Document 64.
- FAO (2005) Land cover classification system: Classification concepts and user manual. Environment and Natural Resources Series 8, Food and Agriculture Organization of the United Nations, Rome.
- Fayad I, Baghdadi N, Guitet S, et al. (2016) Aboveground biomass mapping in French Guiana by combining remote sensing, forest inventories and environmental data. *International Journal of Applied Earth Observation and Geoinformation* 52: 502-514.
<https://doi.org/10.1016/j.jag.2016.07.015>
- Federici S, Tubiello FN, Salvatore M, et al. (2015) New estimates of CO₂ forest emissions and removals: 1990-2015. *Forest Ecology and Management* 352: 89-98.
- <https://doi.org/10.1016/j.foreco.2015.04.022>
- Fernández-Manso A, Fernández-Manso O, Quintano C (2016) SENTINEL-2A red-edge spectral indices suitability for discriminating burn severity. *International Journal of Applied Earth Observation and Geoinformation* 50: 170-175.
<https://doi.org/10.1016/j.jag.2016.03.005>
- Fernández-Manso O, Fernández-Manso A, Quintano C (2014) Estimation of aboveground biomass in Mediterranean forests by statistical modelling of ASTER fraction images. *International Journal of Applied Earth Observation and Geoinformation* 31: 45-56.
<https://doi.org/10.1016/j.jag.2014.03.005>
- Foody GM, Boyd DS, Cutler ME (2003) Predictive relations of tropical forest biomass from Landsat TM data and their transferability between regions. *Remote Sensing of Environment* 85(4): 463-474.
[https://doi.org/10.1016/S0034-4257\(03\)00039-7](https://doi.org/10.1016/S0034-4257(03)00039-7)
- Franklin S, Wulder M, Lavigne M (1996) Automated derivation of geographic window sizes for use in remote sensing digital image texture analysis. *Computers & Geosciences* 22(6): 665-673. [https://doi.org/10.1016/0098-3004\(96\)00009-X](https://doi.org/10.1016/0098-3004(96)00009-X)
- Franklin SE (2001) *Remote sensing for sustainable forest management*. CRC Press.
- Fuchs H, Magdon P, Kleinn C, et al. (2009) Estimating aboveground carbon in a catchment of the Siberian forest tundra: Combining satellite imagery and field inventory. *Remote Sensing of Environment* 113(3): 518-531.
<https://doi.org/10.1016/j.rse.2008.07.017>
- Gairola S, Sharma C, Ghildiyal S, et al. (2011) Live tree biomass and carbon variation along an altitudinal gradient in moist temperate valley slopes of the Garhwal Himalaya (India). *Current Science* 100(12): 1862-1870.
<https://www.jstor.org/stable/24077557>
- Galidaki G, Zianis D, Gitas I, et al. (2017) Vegetation biomass estimation with remote sensing: focus on forest and other wooded land over the Mediterranean ecosystem. *International Journal of Remote Sensing* 38(7): 1940-1966.
<https://doi.org/10.1080/01431161.2016.1266113>
- Gao Y, Lu D, Li G, et al. (2018) Comparative analysis of modeling algorithms for forest aboveground biomass estimation in a subtropical region. *Remote Sensing* 10(4): 627.
<https://doi.org/10.3390/rs10040627>
- Gara TW, Murwira A, Chivhenge E, et al. (2014) Estimating wood volume from canopy area in deciduous woodlands of Zimbabwe. *Southern Forests: A Journal of Forest Science* 76(4): 237-244.
<https://doi.org/10.2989/20702620.2014.965981>
- Gasparri NI, Parmuchi MG, Bono J, et al. (2010) Assessing multi-temporal Landsat 7 ETM+ images for estimating aboveground biomass in subtropical dry forests of Argentina. *Journal of Arid Environments* 74(10): 1262-1270.
<https://doi.org/10.1016/j.jaridenv.2010.04.007>
- Gibbs HK, Brown S, Niles JO, et al. (2007) Monitoring and estimating tropical forest carbon stocks: making REDD a reality. *Environmental Research Letters* 2(4): 045023.
<https://doi.org/10.1088/1748-9326/2/4/045023>
- Godinho S, Guiomar N, Gil A (2018) Estimating tree canopy cover percentage in a mediterranean silvopastoral systems using Sentinel-2A imagery and the stochastic gradient boosting algorithm. *International Journal of Remote Sensing* 39(14): 4640-4662.
<https://doi.org/10.1080/01431161.2017.1399480>
- Goetz SJ, Baccini A, Laporte NT, et al. (2009) Mapping and monitoring carbon stocks with satellite observations: a comparison of methods. *Carbon Balance and Management* 4(1): 2. <https://doi.org/10.1186/1750-0680-4-2>
- Goh J, Miettinen J, Chia AS, et al. (2013) Biomass estimation in humid tropical forest using a combination of ALOS PALSAR and SPOT 5 satellite imagery. *Asian Journal of Geoinformatics* 13 (4): 1-10
- Gosain BG (2016) An Assessment of C-stock and Soil physicochemical properties in standing dead trees of Pine (*Pinus roxburghii* Sargent) forests in a Mountain Watershed Kumaun Himalaya, India. *International Journal of Multidisciplinary Research and Development* 3(4): 279-286.
<https://doi.org/10.13140/RG.2.1.1627.2243>
- Govender M, Chetty K, Bulcock H (2007) A review of

- hyperspectral remote sensing and its application in vegetation and water resource studies. *Water SA* 33(2): 145-152.
<https://doi.org/10.4314/wsa.v33i2.49049>
- Güneralp I, Filippi AM, Randall J (2014) Estimation of floodplain aboveground biomass using multispectral remote sensing and nonparametric modeling. *International Journal of Applied Earth Observation and Geoinformation* 33: 119-126.
<https://doi.org/10.1016/j.jag.2014.05.004>
- Günlü A, Ercanlı I, Başkent E, et al. (2014) Estimating aboveground biomass using Landsat TM imagery: A case study of Anatolian Crimean pine forests in Turkey. *Annals of Forest Research* 57(2): 289-298.
<https://doi.org/10.15287/afr.2014.278>
- Guyot G, Baret F, Major D (1988) High spectral resolution: Determination of spectral shifts between the red and the near infrared. *International Archives of Photogrammetry and Remote Sensing* 11: 750-760.
<https://hal.inrae.fr/hal-02853563>
- Hall FG, Bergen K, Blair JB, et al. (2011) Characterizing 3D vegetation structure from space: Mission requirements. *Remote Sensing of Environment* 115(11): 2753-2775.
<https://doi.org/10.1016/j.rse.2011.01.024>
- Haralick RM, Shanmugam K, Dinstein IH (1973) Textural features for image classification. *IEEE Transactions on Systems, Man, and Cybernetics* 3(6): 610-621.
<https://doi.org/10.1109/TSMC.1973.4309314>
- Harmon ME, Hua C (1991) Coarse woody debris dynamics in two old-growth ecosystems. *BioScience* 41(9): 604-610.
<https://doi.org/10.2307/1311697>
- Heiskanen J (2006) Estimating aboveground tree biomass and leaf area index in a mountain birch forest using ASTER satellite data. *International Journal of Remote Sensing* 27(6): 1135-1158. <https://doi.org/10.1080/01431160500353858>
- Huete A, Keita F, Thome K, et al. (1999) A light aircraft radiometric package for MODLAND quick airborne looks (MQUALS). *EOS Earth Observer* 11(1): 22-25.
- Huete AR (1988) A soil-adjusted vegetation index (SAVI). *Remote Sens Environ* 25(3): 295-309.
[https://doi.org/10.1016/0034-4257\(88\)90106-X](https://doi.org/10.1016/0034-4257(88)90106-X)
- Kasischke ES, Goetz S, Hansen MC, et al. (2014) Remote Sensing for Natural Resource Management and Environmental Monitoring. Manual of Remote Sensing. de Susan, L. Ustin (Ed.), Hoboken, NJ: John Wiley & Sons, c2004. New York, USA.
- Keenan RJ, Reams GA, Achard F, et al. (2015) Dynamics of global forest area: Results from the FAO Global Forest Resources Assessment 2015. *Forest Ecology and Management* 352: 9-20. <https://doi.org/10.1016/j.foreco.2015.06.014>
- Kelsey KC, Neff JC (2014) Estimates of aboveground biomass from texture analysis of Landsat imagery. *Remote Sensing* 6(7):6407-6422. <https://doi.org/10.3390/rs6076407>
- Kumar KK, Nagai M, Witayangkurn A, et al. (2016) Above ground biomass assessment from combined optical and SAR remote sensing data in Surat Thani Province, Thailand. *Journal of Geographic Information System* 8: 506.
<https://doi.org/10.4236/jgis.2016.84042>
- Kumar L, Mutanga O (2017) Remote sensing of above-ground biomass. *Remote Sensing* 9(9): 935.
<https://doi.org/10.3390/rs9090935>
- Kumar L, Sinha P, Taylor S, et al. (2015) Review of the use of remote sensing for biomass estimation to support renewable energy generation. *Journal of Applied Remote Sensing* 9(1): 097696. <https://doi.org/10.1117/1.JRS.9.097696>
- Kumar P, Ghose M (2017) Remote sensing-derived spectral vegetation indices and forest carbon: testing the validity of models in mountainous terrain covered with high biodiversity. *Current Science* 112(10): 2043-2050.
<https://doi.org/10.18520/cs/v112/i10/2043-2050>
- Laurin GV, Balling J, Corona P, et al. (2018) Above-ground biomass prediction by Sentinel-1 multitemporal data in central Italy with integration of ALOS2 and Sentinel-2 data. *Journal of Applied Remote Sensing* 12(1): 016008.
<https://doi.org/10.1117/1.JRS.12.016008>
- Lefsky M, Cohen W, Spies T (2001) An evaluation of alternate remote sensing products for forest inventory, monitoring, and mapping of Douglas-fir forests in western Oregon. *Canadian Journal of Forest Research* 31(1): 78-87.
<https://doi.org/10.1139/x00-142>
- Li M, Tan Y, Pan J, et al. (2008) Modeling forest aboveground biomass by combining spectrum, textures and topographic features. *Frontiers of Forestry in China* 3(1): 10-15.
<https://doi.org/10.1007/s11461-008-0013-z>
- Liu Y, Gong W, Xing Y, et al. (2019) Estimation of the forest stand mean height and aboveground biomass in Northeast China using SAR Sentinel-1B, multispectral Sentinel-2A, and DEM imagery. *ISPRS Journal of Photogrammetry and Remote Sensing* 151: 277-289.
<https://doi.org/10.1016/j.isprsjprs.2019.03.016>
- Lopez-Serrano PM, Lopez-Sanchez CA, Diaz-Varela RA, et al. (2015) Estimating biomass of mixed and uneven-aged forests using spectral data and a hybrid model combining regression trees and linear models. *iForest-Biogeosciences and Forestry* 9(2): 226-234. <https://doi.org/10.3832/ifor1504-008>
- Lu D (2005) Aboveground biomass estimation using Landsat TM data in the Brazilian Amazon. *International Journal of Remote Sensing* 26(12): 2509-2525.
<https://doi.org/10.1080/01431160500142145>
- Lu D (2006) The potential and challenge of remote sensing-based biomass estimation. *International Journal of Remote Sensing* 27(7): 1297-1328.
<https://doi.org/10.1080/01431160500486732>
- Lu D, Batistella M (2005) Exploring TM image texture and its relationships with biomass estimation in Rondônia, Brazilian Amazon. *Acta Amazonica* 35(2): 249-257.
<https://doi.org/10.1590/S0044-59672005000200015>
- Lu D, Chen Q, Wang G, et al. (2016) A survey of remote sensing-based aboveground biomass estimation methods in forest ecosystems. *International Journal of Digital Earth* 9(1): 63-105. <https://doi.org/10.1080/17538947.2014.990526>
- Lu D, Mausel P, Brondizio E, et al. (2004) Relationships between forest stand parameters and Landsat TM spectral responses in the Brazilian Amazon Basin. *Forest Ecology and Management* 198(1): 149-167.
<https://doi.org/10.1016/j.foreco.2004.03.048>
- Maack J, Kattenborn T, Fassnacht FE, et al. (2015) Modeling forest biomass using very-high-resolution data—Combining textural, spectral and photogrammetric predictors derived from spaceborne stereo images. *European Journal of Remote Sensing* 48(1): 245-261.
<https://doi.org/10.5721/EuJRS20154814>
- Majasalmi T, Rautiainen M (2016) The potential of Sentinel-2 data for estimating biophysical variables in a boreal forest: a simulation study. *Remote Sensing Letters* 7(5): 427-436.
<https://doi.org/10.1080/2150704X.2016.1149251>
- Malhi Y, Meir P, Brown S (2002) Forests, carbon and global climate. *Philosophical Transactions of the Royal Society of London Series A: Mathematical, Physical and Engineering Sciences* 360(1797): 1567-1591.
<https://doi.org/10.1098/rsta.2002.1020>
- Marceau DJ, Howarth PJ, Dubois J-MM, et al. (1990) Evaluation of the grey-level co-occurrence matrix method for land-cover classification using SPOT imagery. *IEEE Transactions on Geoscience and Remote Sensing* 28(4): 513-519. <https://doi.org/10.1109/TGRS.1990.572937>
- Mathieu R, Naidoo L, Cho MA, et al. (2013) Toward structural assessment of semi-arid African savannahs and woodlands: The potential of multitemporal polarimetric RADARSAT-2 fine beam images. *Remote Sensing of Environment* 138: 215-231. <https://doi.org/10.1016/j.rse.2013.07.011>
- Meng S, Pang Y, Zhang Z, et al. (2016) Mapping aboveground biomass using texture indices from aerial photos in a temperate forest of Northeastern China. *Remote Sensing* 8(3): 230. <https://doi.org/10.3390/rs8030230>
- Navarro G, Caballero I, Silva G, et al. (2017) Evaluation of forest fire on Madeira Island using Sentinel-2A MSI imagery. *International Journal of Applied Earth Observation and Geoinformation* 58: 97-106.
<https://doi.org/10.1016/j.jag.2017.02.003>
- Nichol JE, Sarker MLR (2011) Improved biomass estimation using the texture parameters of two high-resolution optical sensors. *IEEE Transactions on Geoscience and Remote Sensing* 49(3): 930-948.

- <https://doi.org/10.1109/TGRS.2010.2068574>
- Nizami SM (2012) The inventory of the carbon stocks in sub tropical forests of Pakistan for reporting under Kyoto Protocol. *Journal of Forestry Research* 23(3): 377-384.
<https://doi.org/10.1007/s11676-012-0273-1>
- Nuthammachot N, Askar A, Stratoulias D, et al. (2020) Combined use of Sentinel-1 and Sentinel-2 data for improving above-ground biomass estimation. *Geocarto International* 1-11. <https://doi.org/10.1080/10106049.2020.1726507>
- Nuthammachot N, Phairuang W, Wicaksono P, et al. (2018) Estimating aboveground biomass on private forest using Sentinel-2 imagery. *Journal of Sensors* 2018: 11.
<https://doi.org/10.1155/2018/6745629>
- Pandit S, Tsuyuki S, Dube T (2018) Estimating above-ground biomass in Subtropical buffer zone community forests, Nepal, using Sentinel 2 data. *Remote Sensing* 10(4): 601.
<https://doi.org/10.3390/rs10040601>
- Pandit S, Tsuyuki S, Dube T (2019) Exploring the inclusion of Sentinel-2 MSI texture metrics in above-ground biomass estimation in the community forest of Nepal. *Geocarto International*. <https://doi.org/10.1080/10106049.2019.1588390>
- Pearson T, Walker S, Brown S (2005) Sourcebook for land use, land-use change and forestry projects. Biocarbon Fund and Winrock International.
- Persson HJ (2016) Estimation of boreal forest attributes from very high resolution Pléiades data. *Remote Sensing* 8(9): 736.
<https://doi.org/10.3390/rs8090736>
- Pham TD, Le NN, Ha NT, et al. (2020) Estimating mangrove above-ground biomass using extreme gradient boosting decision trees algorithm with fused Sentinel-2 and ALOS-2 PALSAR-2 data in Can Gio Biosphere Reserve, Vietnam. *Remote Sensing* 12(5): 777.
<https://doi.org/10.3390/rs12050777>
- Pham TD, Yoshino K, Le NN, et al. (2018) Estimating aboveground biomass of a mangrove plantation on the Northern coast of Vietnam using machine learning techniques with an integration of ALOS-2 PALSAR-2 and Sentinel-2A data. *International Journal of Remote Sensing* 39(22): 7761-7788. <https://doi.org/10.1080/01431161.2018.1471544>
- Pinty B, Verstraete M (1992) GEMI: a non-linear index to monitor global vegetation from satellites. *Plant Ecology* 101(1): 15-20. <https://doi.org/10.1007/BF00031911>
- Plaza A, Benediktsson JA, Boardman JW, et al. (2009) Recent advances in techniques for hyperspectral image processing. *Remote Sensing of Environment* 113: 110-122.
<https://doi.org/10.1016/j.rse.2007.07.028>
- Ramoelo A, Cho M, Mathieu R, et al. (2015) Potential of Sentinel-2 spectral configuration to assess rangeland quality. *Journal of Applied Remote Sensing* 9(1): 094096.
<https://doi.org/10.1117/1.JRS.9.094096>
- Rana B, Singh S, Singh R (1988) Biomass and productivity of Chir pine (*Pinus roxburghii* Sarg.) forest in central Himalaya. *Proceedings of Indian National Science Academy* 54: 71-74.
- Ravindranath N, Sathaye JA (2002) Climate change: Vulnerability, impacts and adaptation. In: Climate Change and Developing Countries, vol 11. Springer, pp 63-95.
https://doi.org/10.1007/0-306-47980-X_4
- Rodríguez-Veiga P, Wheeler J, Louis V, et al. (2017) Quantifying forest biomass carbon stocks from space. *Current Forestry Reports* 3(1): 1-18. <https://doi.org/10.1007/s40725-017-0052-5>
- Rousel J, Haas R, Schell J, et al. (1973) Monitoring vegetation systems in the great plains with ERTS. In: Proceedings of the Third Earth Resources Technology Satellite-1 Symposium; NASA SP-351: 309-317.
- Safari A, Sohrabi H (2016) Ability of Landsat-8 OLI derived texture metrics in estimating aboveground carbon stocks of coppice Oak Forests. *International Archives of the Photogrammetry, Remote Sensing & Spatial Information Sciences* 41.
<https://doi.org/10.5194/isprs-archives-XLI-B8-751-2016>
- Shaheen H, Khan RWA, Hussain K, et al. (2016) Carbon stocks assessment in subtropical forest types of Kashmir Himalayas. *Pakistan Journal of Botany* 48(6): 2351-2357
- Shao Z, Zhang L (2016) Estimating forest aboveground biomass by combining optical and SAR data: a case study in Genhe, Inner Mongolia, China. *Sensors* 16(6): 834.
<https://doi.org/10.3390/s16060834>
- Sharma C, Baduni N (2000) Structural attributes and growing stock variations on different aspects of high Himalayan and Siwalik chir pine forests. *Journal of Tropical Forest Science* 12(3): 482-492. <https://www.jstor.org/stable/23616272>
- Sharma CM, Baduni NP, Gairola S, et al. (2010) Tree diversity and carbon stocks of some major forest types of Garhwal Himalaya, India. *Forest Ecology and Management* 260(12): 2170-2179. <https://doi.org/10.1016/j.foreco.2010.09.014>
- Sibanda M, Mutanga O, Rouget M (2015) Examining the potential of Sentinel-2 MSI spectral resolution in quantifying above ground biomass across different fertilizer treatments. *ISPRS Journal of Photogrammetry and Remote Sensing* 110: 55-65. <https://doi.org/10.1016/j.isprsjprs.2015.10.005>
- Siddiqui K (1997) Asia-Pacific Forestry Sector Outlook Study. Country Report—Pakistan. Working paper no: APFSOS/WP/11 Food and Agriculture Organization of the United Nations, Forestry Policy and Planning Division, Rome, regional Office for Asia and the Pacific, Bangkok.
- Steiner M (2000) Satellite estimation of tropical secondary forest above-ground biomass: data from Brazil and Bolivia. *International Journal of Remote Sensing* 21(6-7): 1139-1157.
<https://doi.org/10.1080/014311600210119>
- Tian X, Su Z, Chen E, et al. (2012) Estimation of forest above-ground biomass using multi-parameter remote sensing data over a cold and arid area. *International Journal of Applied Earth Observation and Geoinformation* 17(1): 102-110.
<https://doi.org/10.1016/j.jag.2012.03.007>
- Tucker CJ (1979) Red and photographic infrared linear combinations for monitoring vegetation. *Remote Sensing of Environment* 8(2): 127-150.
[https://doi.org/10.1016/0034-4257\(79\)90013-0](https://doi.org/10.1016/0034-4257(79)90013-0)
- Van Noordwijk M, Cerri C, Woerner PL, et al. (1997) Soil carbon dynamics in the humid tropical forest zone. *Geoderma* 79(1-4): 187-225. [https://doi.org/10.1016/S0016-7061\(97\)00042-6](https://doi.org/10.1016/S0016-7061(97)00042-6)
- Vicharnakorn P, Shrestha RP, Nagai M, et al. (2014) Carbon stock assessment using remote sensing and forest inventory data in Savannakhet, Lao PDR. *Remote Sensing* 6(6): 5452-5479. <https://doi.org/10.3390/rs6065452>
- Vikrant K, Chauhan D (2014) Carbon stock estimation in standing tree of Chir pine and Banj Oak pure forest in two Van Panchayats forest of Garhwal Himalaya. *Journal of Earth Science & Climatic Change* 5(10): 1-3.
<http://doi.org/10.4172/2157-7617.1000240>
- Wani AA, Joshi PK, Singh O (2015) Estimating biomass and carbon mitigation of temperate coniferous forests using spectral modeling and field inventory data. *Ecological Informatics* 25: 63-70.
<https://doi.org/10.1016/j.ecoinf.2014.12.003>
- Wijaya A, Kusnadi S, Gloaguen R, et al. (2010) Improved strategy for estimating stem volume and forest biomass using moderate resolution remote sensing data and GIS. *Journal of Forestry Research* 21(1): 1-12.
<https://doi.org/10.1007/s11676-010-0001-7>
- Yohannes H, Soromessa T, Argaw M (2015) Carbon stock analysis along slope and slope aspect gradient in Gedo Forest: implications for climate change mitigation. *Journal of Earth Science and Climate Change* 6(305): 2.
<https://doi.org/10.4172/2157-7617.1000305>
- Zheng D, Rademacher J, Chen J, et al. (2004) Estimating aboveground biomass using Landsat 7 ETM+ data across a managed landscape in northern Wisconsin, USA. *Remote Sensing of Environment* 93(3): 402-411.
<https://doi.org/10.1016/j.rse.2004.08.008>
- Zhu X, Liu D (2015) Improving forest aboveground biomass estimation using seasonal Landsat NDVI time-series. *ISPRS Journal of Photogrammetry and Remote Sensing* 102: 222-231. <https://doi.org/10.1016/j.isprsjprs.2014.08.014>